RESEARCH ARTICLE
PLANETARY SCIENCES

Earth and Planetary Physics
7: 615–619, 2023
doi: 10.26464/epp2023084

Determining the moment of inertia of triaxial Mars with updated global gravity models

ChangYi Xu*, and Yan Jiang

Institute of Geology and Geophysics, Chinese Academy of Sciences, Beijing 100029, China

Key Points:

- In this study, we determined the principal moments of inertia for Mars and its core using recently updated global gravity models.
- The principal moments of inertia for Mars were $A = 2.66589 \times 10^{36}$ kg·m^2, $B = 2.66775 \times 10^{36}$ kg·m^2, and $C = 2.68125 \times 10^{36}$ kg·m^2.
- The determined core portion of this PMI is 5.47%, which is critical for investigating core density and size, and the free core nutation of Mars.

Citation: Xu, C. Y., and Jiang, Y. (2023). Determining the moment of inertia of triaxial Mars with updated global gravity models. *Earth Planet. Phys.*, *7*(6), 615–619. http://doi.org/10.26464/epp2023084

Abstract: The principal moments of inertia (PMIs) with the principal axes are usually taken as the dynamic figure parameters of Mars; they can be deduced from satellite-observed degree-two gravitational potentials in recent global gravity models and from the dynamic ellipticities resulting from precession observations. These PMIs are natural and significant for the geodetic, geophysical, and geodynamic problems of Mars, which are functions of internal density distributions. In this study, a closed and concise formula for determining the PMIs of the entire planet and its core was developed based on the second invariants of gravity and a multipole expansion. We deduced the polar oblateness J_2 and the equatorial ellipticity J_{22} of Mars to be 1.9566×10^{-3} and 6.3106×10^{-5}, respectively. The preferred principal moments of inertia of Mars are $A = 2.66589 \times 10^{36}$ kg·m^2, $B = 2.66775 \times 10^{36}$ kg·m^2, and $C = 2.68125 \times 10^{36}$ kg·m^2. These values indicate that Mar is slightly triaxial. The equatorial principal moment of inertia of the Martian core is 1.46008×10^{35} kg·m^2, accounting for ~5.47% of the planet's PMI; this result is critical for investigating the density and size of the core of Mars, and the planet's free core nutation.

Keywords: Mars; principal moment of inertia; dynamic ellipticity; Chandler wobble; core density and size

1. Introduction

The principal moments of inertia (PMIs) of Mars are a function of the planet's internal density distributions; during the entire exploration history of the planet, they have been treated as its predominant parameters. PMIs are usually represented by *A*, *B*, and *C;* the mean moment of inertia is defined as one-third of their trace. *A* and *B* are the PMI's equatorial components; *C* is the polar principal PMI. These parameters are essential for constraining the planet's layer structures and solidification (e.g., Bills and James, 1999), its hydrostatic state with internal dynamic processes (e.g., Chambat et al., 2010), and the planet's rotation dynamics, including its Chandler wobble and free core nutation (e.g., Van Hoolst et al., 2000; Dehant et al., 2006; Konopliv et al., 2020).

The PMIs of Mars are still not completely determined because of limited observations and have been represented only by the polar principal moment *C*. Under the assumption of hydrostatic equilibrium, *C* can be approximated using the Darwin–Radau relationship (e.g., Sohl et al., 2005). Moreover, *C* can be derived from the observation of the Martian precession if we treat Mars as a rigid body (e.g., Yoder and Standish, 1997). These two conventional methods are problematic, however, because the status of the hydrostatic equilibrium of Mars is unknown; *C* determined through the Darwin–Radau relationship is always approximate, regardless of how close the value is to the actual value. *C* is proportional to the observed precession rate and is coupled with dynamic oblateness, which means that *C* will be affected by observation errors.

The PMIs of Mars may also be deduced from the eigenvalues of the moment of inertia tensor if that eigenvalue–eigenvector problem is solved. However, the PMIs of Mars have not been completely determined because of the non-uniqueness of gravitational inversion. Another independent observation is a planet's precession (as in the case of Mars) or physical libration (for example, Mercury) (see Section 2). With the accumulation of observational data, the global gravity model of Mars has been updated (Genova et al., 2016; Konopliv et al., 2016, 2020), providing an excellent opportunity to precisely determine the PMIs of Mars. Moreover, a complete and precise determination of the PMIs of Mars is crucial for studies of the planet's interior density structure, its Chandler wobble (CW), and its free core nutation (FCN) (e.g., Van Hoolst et al., 2000).

Because of the nature of PMIs, knowledge of a planet's core portion can provide strong constraints to its density and size,

Correspondence to: C. Y. Xu, xucy@mail.iggcas.ac.cn
Received 21 AUG 2023; Accepted 03 OCT 2023.
First Published online 11 OCT 2023.

which are important to the investigation of its accretion and evolution, and the history of its geodynamo (Brennan et al., 2020). Moreover, the PMIs of the Martian core can influence the eigenperiods of the planet's FCN and CW (e.g., Van Hoolst et al., 2000). Thus, observation of the period of the FCN or the CW can help determine the PMIs of the Martian core, which can be further adapted to invert the density and size of the core. The rotation and interior structure experiment (RISE) of the InSight mission was designed to detect the FCN of Mars (Folkner et al., 2018).

The goal of this study is to determine the principal moments of inertia of Mars and the PMIs of the planet's fluid core as precisely as possible, by applying recently updated global gravity models (GGM3, MRO120D, and MRO120F) to the most accurate precession observations. Since the temporal component of the gravity model did not significantly affect our estimation, we did not consider it. In the absence of H_D (so-called precession constant), we also propose an alternative method to estimate the PMIs for other terrestrial planets and their satellites, such as Mercury and the Moon.

2. PMIs with Global Gravity Models

2.1 Moment of Inertia Theory

The moment of inertia tensor of an arbitrary celestial body is geodetically related to the degree-2 gravitational potential in the terrestrial reference frame (see Figure 1), which can be expressed as (e.g., Chao and Gross, 1987):

$$V_2 = \frac{GM}{R_a}\sum_{m=0}^{2}\left(\bar{C}_{2m}\cos m\lambda + \bar{S}_{2m}\sin m\lambda\right)\bar{P}_{2m}(\cos\theta), \tag{1}$$

where M is the body mass and R_a is the mean radius. $\bar{C}_{2m}$ and $\bar{S}_{2m}$ are the degree-2 normalized harmonic coefficients for the potential, *i.e.*, the Stokes coefficients, which can be deduced from the global gravity model thanks to the radio tracking data of Mars orbiters and landers. $\bar{P}_{2m}(\cos\theta)$ is the normalized Legendre function. (θ, λ) are the co-latitude and longitude of the field point, respectively.

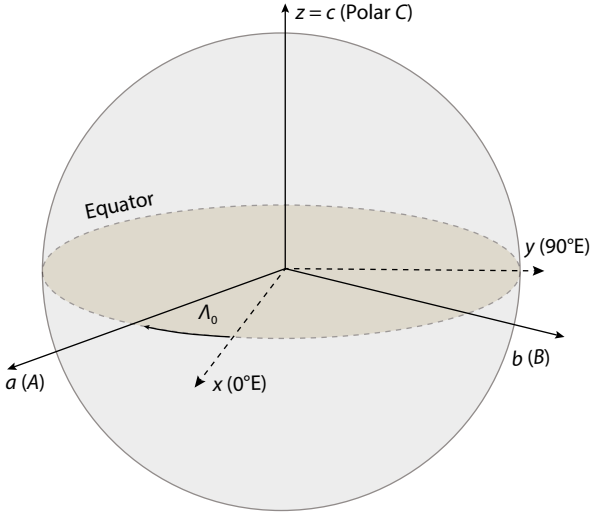

Figure 1. The three principal moments of inertia (A, B, C) with their principal axes (a-b-c) of Mars in the terrestrial reference frame (x-y-z). The c points to the north pole, which is virtually within the Martian spin axis or the z-axis by neglecting the small departure of the polar motion of Mars. Λ_0 is the east longitude of the a-axis expressed in the terrestrial reference frame.

The moment of inertia tensor $\boldsymbol{I}$ is directly related to the degree-2 Stokes coefficients using MacCullagh's formula (e.g., Heiskanen and Moritz, 1967) or multipole expansion (Chao and Shih, 2021):

$$\begin{aligned}
\bar{C}_{20} &= (I_{11} + I_{22} - 2I_{33})/\left(2\sqrt{5}MR_a^2\right),\\
\bar{C}_{21} &= -\sqrt{3}I_{13}/\left(\sqrt{5}MR_a^2\right),\\
\bar{S}_{21} &= -\sqrt{3}I_{23}/\left(\sqrt{5}MR_a^2\right),\\
\bar{C}_{22} &= \sqrt{3}(I_{22} - I_{11})/\left(2\sqrt{5}MR_a^2\right),\\
\bar{S}_{22} &= -\sqrt{3}I_{12}/\left(\sqrt{5}MR_a^2\right).
\end{aligned} \tag{2}$$

A detailed derivation of Equation (2) with normalized factors can be found in Chao and Gross (1987) and Xu CY et al. (2014).

The degree-2 potential is given by the Principal Axial Frame (PAF, see Figure 1) (e.g., Bills and Rubincam, 1995; Marchenko and Schwintzer, 2003; Chen W et al., 2015):

$$V_2 = \frac{GMR_a^2}{r_l^3}\left[A_{20}P_{20}(\cos\theta_l) + A_{22}\sin 2\lambda_l P_{22}(\cos\theta_l)\right]. \tag{3}$$

With

$$\begin{aligned}
A_{20} &= -\frac{C - (A+B)/2}{\sqrt{5}MR_a^2},\\
A_{22} &= \frac{\sqrt{15}(B-A)}{10MR_a^2},
\end{aligned} \tag{4}$$

where r_l is the distance between the field point and the coordinate origin in the PAF, and θ_l is the colatitude in the PAF. A, B, and C are the three principal moments of Mars; A, and B represent the equatorial components, and C represents the polar PMI. A_{20} and A_{22} are the coefficients of the degree-2 potential in the PAF, which are introduced to avoid ambiguity. Hence the polar oblateness J_2 and the equatorial ellipticity J_{22} are written as:

$$\begin{aligned}
J_2 &= -\sqrt{5}A_{20},\\
J_{22} &= \frac{\sqrt{15}}{6}A_{22},
\end{aligned} \tag{5}$$

where J_2 is the polar oblateness, which represents the difference between the polar PMI C and the mean equatorial PMI $\left(\frac{A+B}{2}\right)$, and J_{22} is the equatorial ellipticity, which reflects the difference between A and B. Notably, the differences between the coefficients C_{2m}, S_{2m}, A_{20}, A_{22}, J_2, and J_{22} are easily mixed; they are defined in the different reference frames. The moment of inertia (I_{ij}) derived from the degree-two Stokes coefficients is not the PMIs (A, B, C). A, B, and C can be deduced only by solving the eigenvalue–eigenvector problem of Equation (2).

Notably, there are only five degree-two coefficients with six independent components in $\boldsymbol{I}$ in Equation (2) and only two coefficients with three independent components in Equation (3) (due to gravitational inversion non-uniqueness). To uniquely determine PMIs, one more independent observation is needed: the dynamic ellipticity (or so-called precession constant) $H_D = \frac{C - (A+B)/2}{C}$ in the

case of Earth and Mars.

Once A_{20} and A_{22} are determined, we can get the principal inertial moments with H_D in the case of Mars:

$$\begin{aligned} A &= \sqrt{5}MR_a^2\left[\left(1-\frac{1}{H_D}\right)A_{20}-\frac{A_{22}}{\sqrt{3}}\right],\\ B &= \sqrt{5}MR_a^2\left[\left(1-\frac{1}{H_D}\right)A_{20}+\frac{A_{22}}{\sqrt{3}}\right],\\ C &= -\sqrt{5}MR_a^2\frac{A_{20}}{H_D}. \end{aligned} \tag{6}$$

Then, we can obtain the relative moment differences, which are called three compliances (α, β, γ) of PMIs as follows:

$$\begin{aligned} \alpha &= \frac{(C-B)}{A},\\ \beta &= \frac{(C-A)}{B},\\ \gamma &= \frac{(B-A)}{C} = \frac{-2H_DA_{22}}{\sqrt{3}A_{20}}. \end{aligned} \tag{7}$$

From Equation (7), we can also derive the principal inertial moments through α, β, γ with the absence of H_D, which will be in the case of Moon and Mercury. β, γ are also called the physical latitudinal libration and longitudinal libration parameters, respectively, and can be determined for the Moon from Lunar laser ranging (e.g., Williams et al., 2014) and for the Mercury from its 88-day libration (Margot et al., 2007). However, if the core of a planet is (partially or entirely) fluid, the mantle and core should be decoupled; C_m is then the polar moment of inertia of the mantle. If a solid inner core is present, a small correction to C_m should be included. γ in Equation (7) will be written as:

$$\gamma = \frac{(B-A)}{C_m}\frac{C_m}{C} = \frac{-2H_DA_{22}}{\sqrt{3}A_{20}}. \tag{8}$$

In this case, we can further investigate the ratio of core–mantle coupling $\left(\frac{C_m}{C}\right)$, or the solid part of the PMIs of a terrestrial planet. If we have observations of α, β, γ, we can deduce the period of the Euler motion of a rigid Mars P^{rigid} as follows (e.g., Xu CY et al., 2014; Rekier et al., 2022):

$$P^{\text{rigid}} = \frac{2\pi}{\omega}\sqrt{\frac{AB}{(C-A)(C-B)}} = \frac{2\pi}{\omega}(\alpha\beta)^{\frac{-1}{2}}. \tag{9}$$

In Equation (9), ω is the spin rate of the Mars.

2.2 PMIs of the Whole of Mars

The global gravity model of Mars was updated in terms of Stokes coefficients using radio-tracking data from historical orbiters and landers. Data from the Mars global surveyor (MGS), Mars Reconnaissance Orbiter (MRO), and landers Viking 1, Opportunity, and InSight, have resulted in different models based on the missions' different approaches to data collection. In this study, we have adopted three tide-free degree-two coefficients of global gravity solutions, named GGM3 (Genova et al., 2016), MRO120D (Konopliv et al., 2016), and MRO120F (Konopliv et al., 2020), which are listed in Table 1.

In determining a global gravity model, the mean equatorial radius R_e is typically adopted; for Mars, R_e = 3396 km. The mean radius R_a of Mars is 3389.508 km (Smith et al., 1999). The bulk mean density of Mars is affected by the uncertainty of the gravitational constant G. Hence, we have adopted the value of G from Tiesinga et al. (2021), as recommended by the Committee on Data for Science and Technology (CODATA). The mass and bulk mean density of Mars using different global gravity models were determined to be $M = 6.41735 \times 10^{23}$ kg, and 3934 kg/m^3, respectively.

According to Equations (4) and (5), we can obtain the potential coefficients in the PAF, polar oblateness, and equatorial ellipticity from the different models as follows:

From Table 2, it is clear that Mars is triaxial. The determined J_2 and J_{22} are fundamental for investigating the hydrostatic state of Mars (e.g., Chambat et al., 2010) and constraining the planet's bulk composition from mineral physical simulations (e.g., Wang Y et al., 2013) based on the assumption of hydrostatic equilibrium. This has been discussed from the perspective of possible non-hydrostatic sources in the Martian mantle.

Except for Earth, the dynamic ellipticity of other terrestrial planets is seldom considered. For Mars, the dynamical ellipticity H_D is

Table 1. The standard gravitational constant and degree-two coefficients of Mars, from selected global gravity models.

Coefficients	GMM3	MRO120D	MRO120F
$GM\times10^{13}$ (m^3/s^2)	4.2828372854187757	4.282837581575610	4.28283756639565
$C_{20}\times10^{-4}$	−8.7502113235452894	−8.750220924537	−8.7502198198940
$C_{21}\times10^{-10}$	5.9031495993080755	4.022333306382	3.7546373236670
$S_{21}\times10^{-11}$	−4.9433617424482412	2.303183853552	2.2000860908190
$C_{22}\times10^{-5}$	−8.4635903869414677	−8.463302655983	−8.4632835759060
$S_{22}\times10^{-5}$	4.8934625860229178	4.893941832167	4.8939759011920

Table 2. Degree-2 coefficients in the PAF, the polar oblateness, and the equatorial ellipticity, according to selected global gravity models.

Model ID	A_{20} ($\times10^{-3}$)	A_{22} ($\times10^{-4}$)	J_2 ($\times10^{-3}$)	J_{22} ($\times10^{-5}$)
GGM3	−0.87502113	0.97764175	1.956606734	6.310650334
MRO120D	−0.87502209	0.97764083	1.956608881	6.310644397
MRO120F	−0.87502198	0.97764088	1.956608634	6.310644744

Table 3. Principal moments of inertia and three compliances, computed from selected global gravity models.

Model ID	A (10^{36} kg·m^2)	B (10^{36} kg·m^2)	C (10^{36}kg·m^2)	α (10^{-2})	β (10^{-2})	γ (10^{-3})
GGM3	2.665890032	2.667751104	2.681246128	0.506210817	0.575619516	0.694107216
MRO120D	2.665893143	2.667754214	2.681249255	0.506210888	0.575619446	0.694105801
MRO120F	2.665892797	2.667753868	2.681248907	0.506210882	0.575619452	0.694105927

taken from Baland et al. (2020) and $H_D = 5.38017 \times 10^{-3}$, which can meet the current determination of the precession rate of Mars (e.g., Konopliv et al., 2020). Based on Equation (6), the principal inertial moments are listed in Table 3.

Using the determined A, B, and C, we can obtain the mean inertial moment of Mars, $T = (A+B+C)/3$, and then we can precisely obtain the mean inertial moment factor of Mars rather than estimating it approximately from two conventional methods: the Darwin–Radau relationship, and measurements of Martian precession.

2.3 Dynamic Figure Parameters of Internal Layers

Unlike the whole of Mars, whose moment of inertia is directly computed from gravity observations, the principal internal moments of the core can be deduced only from the assumption of hydrostatic equilibrium or from observations of the FCN or the CW with the influence of its fluidity. Based on observations of the CW period of Mars (Konopliv et al., 2020), we used the following relation to compute the equatorial principal moments of the Martian core:

$$P_{\mathrm{CW}}^{\mathrm{obs}} = P^{\mathrm{rigid}}\left(1-\frac{k_2}{k_s}\right)^{-1}\left[1-\left(\frac{A_c B_c}{AB}\right)^{\frac{1}{2}}\right], \tag{10}$$

where the observed period of $P_{\mathrm{CW}}^{\mathrm{obs}}$ is ~206.9 days (Konopliv et al., 2020); k_2 is the Love number with allowance for frequency dependence; and k_s is the secular Love number that characterizes Mars's anelasticity ($k_s = \frac{3J_2\overline{g}}{\omega^2 R_a} = 1.2862$), which can be theoretically deduced from the above estimates. Based on the determined PMIs, we deduce the period of the Euler motion of a rigid Mars (~190.07 days). A_c and B_c are the equatorial principal moments of inertia of the Martian core. We can obtain A_c and B_c if the Martian core is assumed to be hydrostatic:

$$A_c = B_c = 1.46008 \times 10^{35}, \tag{11}$$

A_c is in kg·m^2.

This indicates that the equatorial internal moments of the core are ~5.47% of the equatorial internal moments of the whole of Mars. Here, $\frac{A}{A_m} = 1.0579$, where A_m is the equatorial principal moment of inertia of the mantle. The polar principal moment of inertia of core C_c cannot be determined without knowing the dynamic flattening of the core of Mars e_f ($e_f = (C_c - A_c)/A_c$), that is, the dynamic flattening at the core and mantle boundary (CMB). This can be determined by solving Clairaut's equation using the radial– density model of the Martian core.

3. Conclusion and Discussion

In this study, we completely determined the PMIs for the entire planet of Mars and its core using recently updated global gravity models and precession observations. According to Tables 2 and 3, the principal moments of inertia for Mars are $A = 2.66589 \times 10^{36}$ kg·m^2, $B = 2.66775 \times 10^{36}$ kg·m^2, and $C = 2.68125 \times 10^{36}$ kg·m^2. This indicates that Mars is triaxial. If the Martian core is assumed hydrostatic, we can estimate A_c and B_c with the CW of Mars and the absence of dynamic core flattening. The resulting equatorial principal moment of inertia of the Martian core is 1.46008×10^{35} kg·m^2. We believe that our use of updated global gravity models and data from continuous observations of Martian precession have made our PMI estimates the best that are currently available.

Accurately estimated PMIs can strongly constrain the internal structure of Mars, with the advantage of interfaces determined by the InSight seismic record. Our estimations can replace previous physical parameters to refine the interior model of Mars in combination with geochemical data and mineral physical simulations. In particular, the mean moment of inertia ($(A+B+C)/3MR_a^2$), which is the predominant variable for inverting spherically-symmetric layered structures, can be deduced from our new estimation. The PMIs determined for the Martian core can be used to invert its density structure, corresponding to its composition, state, and formation (Brennan et al., 2020).

Our estimated polar oblateness J_2 and equatorial ellipticity J_{22} of Mars are 1.9566×10^{-3} and 6.3106×10^{-5}, respectively. With the given compositions of the Martian mantle, J_2 from mineral physics simulations (e.g., Chambat et al., 2010; Wang Y et al., 2013) can be deduced; comparison to our estimates can reveal the non-hydrostatic portion of the Martian mantle (e.g., Bills and James., 1999). It is important to constrain the mantle mass anomaly that might be induced by the mantle convection (see Forte, 2007 for a review).

These new estimates of PMIs are also important for investigating the rotation dynamics of Mars and the corresponding physical excitations, such as the FCN and the CW (Van Hoolst et al., 2000). As inferred from our results, the ratio of $\frac{A}{A_m}$ can provide a prior constraint for the liquid–core amplification factor, a key factor in the rotation and interior structure experiment (RISE) loaded on the InSight mission (Folkner et al., 2018).

Acknowledgments

All data on global gravity models for Mars are available online from the PDS website (https://pds-geosciences.wustl.edu) as well as via Konopliv et al. (2016), Genova et al. (2016), and Konopliv et al. (2020). This work was supported by the National Key Research and Development Program (2022YFF0503200), the National Natural Science Foundation of China (42274114), and the Key Program of the Institute of Geology and Geophysics, Chinese

Academy of Sciences (IGGCAS-202102). We are grateful to the editor, and two anonymous reviewers for their constructive comments that have greatly improved this manuscript.

References

Baland, R.-M., Yseboodt, M., Le Maistre, S., Rivoldini, A., Van Hoolst, T., and Dehant, V. (2020). The precession and nutations of a rigid Mars. *Celest. Mech. Dyn. Astron.*, *132*(9), 47. https://doi.org/10.1007/s10569-020-09986-0

Bills, B. G., and Rubincam, D. P. (1995). Constraints on density models from radial moments: Applications to Earth, Moon, and Mars. *J. Geophys. Res.*: *Plants*, *100*(E12), 26305–26315. https://doi.org/10.1029/95JE02776

Bills, B. G., and James, T. S. (1999). Moments of inertia and rotational stability of Mars: Lithospheric support of subhydrostatic rotational flattening. *J. Geophys. Res.*: *Planets*, *104*(E4), 9081–9096. https://doi.org/10.1029/1998JE900003

Brennan, M. C., Fischer, R. A., and Irving, J. C. E. (2020). Core formation and geophysical properties of Mars. *Earth Planet. Sci. Lett.*, *530*, 115923. https://doi.org/10.1016/j.epsl.2019.115923

Chambat, F., Ricard, Y., and Valette, B. (2010). Flattening of the Earth: Further from hydrostaticity than previously estimated. *Geophys. J. Int.*, *183*(2), 727–732. https://doi.org/10.1111/j.1365-246X.2010.04771.x

Chao, B. F., and Gross, R. S. (1987). Changes in the Earth's rotation and low - degree gravitational field induced by earthquakes. *Geophys. J. R. Astr. Soc.*, *91*(3), 569–596. https://doi.org/10.1111/j.1365-246X.1987.tb01659.x

Chao, B. F., and Shih, S. A. (2021). Multipole expansion: Unifying formalism for Earth and planetary gravitational dynamics. *Surv. Geophys.*, *42*(4), 803–838. https://doi.org/10.1007/s10712-021-09650-8

Chen, W., Li, J. C., Ray, J., Shen, W. B., and Huang, C. L. (2015). Consistent estimates of the dynamic figure parameters of the earth. *J. Geod.*, *89*(2), 179–188. https://doi.org/10.1007/s00190-014-0768-y

Dehant, V., de Viron, O., Karatekin, O., and Van Hoolst, T. (2006). Excitation of Mars polar motion. *A&A*, *446*(1), 345–355. https://doi.org/10.1051/0004-6361:20053825

Folkner, W. M., Dehant, V., Le Maistre, S., Yseboodt, M., Rivoldini, A., Van Hoolst, T., Asmar, S. W., and Golombek, M. P. (2018). The rotation and interior structure experiment on the InSight mission to Mars. *Space Sci. Rev.*, *214*(5), 100. https://doi.org/10.1007/s11214-018-0530-5

Forte, A. M. (2007). Constraints on seismic models from other disciplines – Implications for mantle dynamics and composition. In G. Schubert (Ed.), *Treatise on Geophysics* (pp. 805-858). Amsterdam: Elsevier. https://doi.org/10.1016/B978-044452748-6.00027-4

Genova, A., Goossens, S., Lemoine, F. G., Mazarico, E., Neumann, G. A., Smith, D. E., and Zuber, M. T. (2016). Seasonal and static gravity field of Mars from MGS, Mars Odyssey and MRO radio science. *Icarus*, *272*, 228–245. https://doi.org/10.1016/j.icarus.2016.02.050

Heiskanen, W. A., and Moritz, H. (1967). *Physical Geodesy*. San Francisco: Freeman and Company.

Konopliv, A. S., Park, R. S., and Folkner, W. M. (2016). An improved JPL Mars gravity field and orientation from Mars orbiter and lander tracking data. *Icarus*, *274*, 253–260. https://doi.org/10.1016/j.icarus.2016.02.052

Konopliv, A. S., Park, R. S., Rivoldini, A., Baland, R.-M., Le Maistre, S., Van Hoolst, T. V., Yseboodt, M., and Dehant, V. (2020). Detection of the Chandler wobble of Mars from orbiting spacecraft. *Geophys. Res. Lett.*, *47*(21), e2020GL090568. https://doi.org/10.1029/2020GL090568

Marchenko, A. N., and Schwintzer, P. (2003). Estimation of the Earth's tensor of inertia from recent global gravity field solutions. *J. Geod.*, *76*(9), 495–509. https://doi.org/10.1007/s00190-002-0280-7

Margot, J. L., Peale, S. J., Jurgens, R. F., Slade, M. A., and Holin, I. V. (2007). Large longitude libration of Mercury reveals a molten core. *Science*, *316*(5825), 710–714. https://doi.org/10.1126/science.1140514

Rekier, J., Chao, B. F., Chen, J. L., Dehant, V., Rosat, S., and Zhu, P. (2022). Earth's rotation: Observations and relation to deep interior. *Surv. Geophys.*, *43*, 149–175. https://doi.org/10.1007/s10712-021-09669-x

Smith, D. E., Zuber, M. T., Solomon, S. C., Phillips, R. J., Head, J. W., Garvin, J. B., Banerdt, W. B., Muhleman, D. O., Pettengill, G. H., ... Duxbury, T. C. (1999). The global topography of Mars and implications for surface evolution. *Science*, *284*(5419), 1495–1503. https://doi.org/10.1126/science.284.5419.1495

Sohl, F., Schubert, G., and Spohn, T. (2005). Geophysical constraints on the composition and structure of the Martian interior. *J. Geophys. Res.*, *110*, E12008. https://doi.org/10.1029/2005JE002520

Tiesinga, E., Mohr, P. J., Newell, D. B., and Taylor, B. N. (2021). CODATA recommended values of the fundamental physical constants: 2018. *Rev. Mod. Phys.*, *93*(2), 025010. https://doi.org/10.1103/RevModPhys.93.025010

Van Hoolst, T., Dehant, V., and Defraigne, P. (2000). Chandler wobble and free core nutation for Mars. *Planet. Space Sci.*, *48*(12-14), 1145–1151. https://doi.org/10.1016/S0032-0633(00)00099-4

Wang, Y., Wen, L. X., and Weidner, D. J. (2013). Composition of Mars constrained using geophysical observations and mineral physics modeling. *Phys. Earth Planet. Inter.*, *224*, 68–76. https://doi.org/10.1016/j.pepi.2013.08.005

Williams, J. G., Konopliv, A. S., Boggs, D. H., Park, R. S., Yuan, D.-N., Lemoine, F. G., Goossens, S., Mazarico, E., Nimmo, F., ... Zuber, M. T. (2014). Lunar interior properties from the GRAIL mission. *J. Geophys. Res.*: *Planets*, *119*(7), 1546–1578. https://doi.org/10.1002/2013JE004559

Xu, C. Y., Sun, W. K., and Chao, B. F. (2014). Formulation of coseismic changes in Earth rotation and low-degree gravity field based on the spherical Earth dislocation theory. *J. Geophys. Res.*: *Solid Earth*, *119*(12), 9031–9041. https://doi.org/10.1002/2014JB011328

Yoder, C. F., and Standish, E. M. (1997). Martian precession and rotation from Viking lander range data. *J. Geophys. Res.*, *102*(E2), 4065–4080. https://doi.org/10.1029/96JE03642